Punjab University
Journal of Mathematics (ISSN 1016-2526)
Vol. 51(2)(2019) pp. 61-78

A Numerical Scheme to Solve an Inverse Problem Related to a Time-Fractional Diffusion-Wave Equation with an Unknown Boundary Condition

Afshin Babaei
Department of Mathematics,
University of Mazandaran, P. O. Box: 47416-95447, Babolsar, Iran.
Email: babaei@umz.ac.ir

Seddigheh Banihashemi
Department of Mathematics,
University of Mazandaran, P. O. Box: 47416-95447, Babolsar, Iran.
Email: s.banihashemi2596@gmail.com

Alireza Mohammadpour
Department of Mathematics,
Islamic Azad University, Babol Branch, Babol, Iran.
Email: mohammadpour@baboliau.ac.ir

Received: 31 January, 2018 / Accepted: 28 March, 2018 / Published online: 15 December, 2018

Abstract. In the present research, a time fractional inverse diffusion-wave problem of finding the inaccessible boundary value, by the input data at an interior point, is investigated. The numerical algorithm is based on the marching finite difference method. Because of ill-posedness of this inverse problem, we apply the mollification regularization technique to obtain a stable numerical solution. It is proven that the numerical scheme is stable and convergent. In the end, the performance of the proposed numerical approach is assessed by some test examples.

AMS (MOS) Subject Classification Codes: 35R30; 65M12; 35R25
Key Words: Time fractional diffusion-wave equation, Inverse problem, Mollification technique, Marching method, Stability analysis.

1. Introduction

In recent decades, employing differential and integral equations to model many phenomena in different branches of engineering and sciences, have been found more attention. Mathematical physics [2, 23], mechanical engineering [9, 12, 15, 24, 31], viscoelastic [3, 16], thermodynamics [14], complex materials [6, 11], heat transfer and distribution [5, 25], network synthesis [26] and mathematical Biosciences [7, 29] are some examples of these disciplines. Some of these models are based on equations with fractional order operators. The fractional diffusion-wave equation is one of these equations that can be obtained from the generalization of the diffusion or wave equation of integer order. This equation is used to describe some anomalous diffusion processes [4, 16]. In some real situations, the boundary data related to the problem cannot be accessible. We only have some additional noisy measured data at an interior point of the domain of the problem. This type of problem is categorized as an inverse problem. The main difficulty in working on these problems is their ill-posedness, that is, some small noise in the input functions may be caused a large error in the solution of the problem [1, 8, 13, 19, 27, 30, 34]. Moreover, finding a numerical approximation for the fractional derivative is an ill-posed process, since the fractional derivative is defined by a nonlocal weak singular integration [21]. As a result, research works on inverse problems related to the time-fractional inverse diffusion-wave equation are very few.

Consider the following equation:

$$D_t^{(\alpha)} u(x,t) = u_{xx}(x,t) + f(x,t), \qquad (x,t) \in \Omega := [0,1] \times [0,1], \tag{1. 1}$$

with the initial and the boundary value conditions

$$u(x,0) = \phi(x),\ u_t(x,0) = \psi(x), \qquad x \in [0,1], \tag{1. 2}$$

$$u(0,t) = \varphi(t),\ u(1,t) = \rho(t), \qquad t \in [0,1], \tag{1. 3}$$

where $f(x,t)$ is the source term and $D_t^{(\alpha)} u(x,t)$ is the Caputo fractional derivative of order $1 < \alpha < 2$ defined as [22]:

$$D_t^{(\alpha)} u(x,t) = \frac{1}{\Gamma(2-\alpha)} \int_0^t \frac{\partial^2 u(x,s)}{\partial s^2} \frac{ds}{(t-s)^{\alpha-1}}, \qquad \alpha \in (1,2).$$

In this study, we are concerned with the inverse problem of approximating the unknown boundary condition $\rho(t)$, while the initial functions $\phi(x)$ and $\psi(x)$ and the boundary condition $\varphi(t)$ are considered as known functions. To determine the set of functions (u, ρ) in the inverse problem (1. 1)-(1. 3), we need a supplementary condition. Here, the condition

$$u(\bar{x},t) = \eta(t), \qquad t \in [0,1], \tag{1. 4}$$

at an interior point $0 < \bar{x} < 1$ is used.

The paper consists of the following sections. In the next section, we separate the problem (1. 1)-(1. 4) into two direct and inverse subproblems, respectively in the domains $0 \le x \le \bar{x}$ and $\bar{x} \le x \le 1$. Afterwards, we apply an implicit finite difference method to obtain the numerical solution of the direct subproblem and a combination of the marching method along with the mollification method to solve the inverse subproblem. In Section 3, it is proven that the numerical procedure is stable and convergent. Finally, in Section 4, numerical examples are provided.

2. Numerical prodecure

2.1. Mollification regularization method

The time-fractional inverse problem with unknown boundary condition is sensitive to the noisy input data and is generally ill-posed [13]. In practice, we have only a perturbed approximation of the input function $\eta(t)$ in the condition (1. 4). Thus, using an appropriate regularization method is necessary to find a stable numerical solution. In this work, we employ the mollification technique. This method is a regularization procedure that stabilizes an ill-posed problem by restoring continuity subject to the data [17, 18, 20, 33]. It uses a convolution of the noisy input data and a smooth function with a parameter, to filter the high-frequency components of the noisy data.

Let $\delta > 0$ and $p > 0$ such that $p\delta < 0.5$. The δ-mollification of an integrable function is based on convolution with the Gaussian kernel

$$\rho_{\delta,p}(t) = \begin{cases} A_p \delta^{-1} exp(-\frac{t^2}{\delta^2}), & |t| \leq p\delta, \\ 0, & |t| > p\delta. \end{cases}$$

where

$$A_p = \Big(\int_{-p}^{p} exp(-s^2) ds \Big)^{-1}.$$

The δ-mollifier $\rho_{\delta,p}$ is a non-negative $C^\infty(-p\delta, p\delta)$ function vanishing outside $(-p\delta, p\delta)$ and satisfying

$$\int_{-p\delta}^{p\delta} \rho_{\delta,p}(t) dt = 1. \tag{2. 5}$$

Now, let $g(t)$ is an integrable function on $I = [0, 1]$ and $t \in I_\delta = [p\delta, 1 - p\delta]$. The δ-mollification of g is defined as

$$\mathcal{J}_\delta g(t) = (\rho_{\delta,p} * g)(t) = \int_{t-p\delta}^{t+p\delta} \rho_{\delta,p}(t-s) g(s) ds.$$

The parameter δ is specified by the generalized cross validation (GCV) criteria [20]. In the rest, we define the mollification of a discrete function.

Suppose $Z = \{1, 2, ..., m\}$, $K = \{t_j : j \in Z\} \subset I$ and $\Delta t = \sup_{j \in Z}(t_{j+1} - t_j)$, satisfying

$$t_{j+1} - t_j > d > 0\,, \quad j \in Z,$$

where m is a positive integer and d is a positive constant. Let $G = \{g(t_j) = g_j : j \in Z\}$ be a discrete function defined on K. We set

$$s_j = \frac{1}{2}(t_j + t_{j+1}), \quad j \in Z.$$

Now, the discrete δ-mollification of G is defined as:

$$\mathcal{J}_\delta G(t) = \sum_{j=-\infty}^{\infty} \Big(\int_{s_{j-1}}^{s_j} \rho_\delta(t-s) ds \Big) g_j.$$

and

$$\begin{aligned} \mathcal{J}_\delta G(t_i) &= \sum_{j=-\infty}^{\infty} \Big(\int_{s_{j-1}}^{s_j} \rho_\delta(t_i - s) ds \Big) g_j \\ &= \sum_{j=-\eta}^{\eta} \Big(\int_{s_{j-1}}^{s_j} \rho_\delta(-y) dy \Big) g_{i+j}, \end{aligned} \tag{2. 6}$$

where $\eta = \left[p\dfrac{\delta}{\Delta t}\right] + 1$. Subject to (2. 5), we obtain

$$\sum_{j=-\infty}^{\infty}\Big(\int_{s_{j-1}}^{s_j}\rho_\delta(t-s)ds\Big) = \int_{-p\delta}^{p\delta}\rho_\delta(s)ds = 1.$$

Theorem 2.1. *Let the functions g and g^ε are uniformly Lipschitz on $\mathbb{R}$ and $\|g-g^\varepsilon\|_\infty \le \varepsilon$, then there exists a constant C, independent of δ, such that*

$$\|\mathcal{J}_\delta g^\varepsilon - g\|_\infty \le C\delta + \varepsilon.$$

Theorem 2.2. *Let the functions g and g^ε are uniformly Lipschitz on $\mathbb{R}$. Also, let $G = \{g_j : j \in Z\}$ and $G^\varepsilon = \{g_j^\varepsilon : j \in Z\}$ be the discrete versions of g and g^ε, which are defined on K, satisfying $\|G - G^\varepsilon\|_\infty \le \varepsilon$. Then*

$$\|D^2(\mathcal{J}_\delta G)(t_j) - D^2(\mathcal{J}_\delta G^\varepsilon)(t_j)\|_\infty \le C\frac{\varepsilon}{\delta^2}, \qquad j \in Z,$$

where D^2 is second-order finite difference operator and C in the above relation is a constant, independent of δ.

The proofs of these theorems can be found in [20].

Theorem 2.3. *Suppose $G = \{g_j : j \in Z\}$ is the discrete version of g, which is defined on K and let a differentiation operator D_δ^2 be defined by the following rule:*

$$D_\delta^2(G) = D^2(\mathcal{J}_\delta G)(t)\Big|_K.$$

Then, there exists a constant C, independent of δ, such that

$$\|D_\delta^2(G)\|_\infty \le \frac{C\|G\|_\infty}{\delta^2(\Delta t)^2}.$$

Proof. According to (2. 6), for $t = t_j \in K$, we have

$$\begin{aligned}
|D_\delta^2(G)| &= \Big|\sum_{j=-\infty}^{\infty}\Big(\int_{s_{j-1}}^{s_j}\frac{\rho_\delta(t+\Delta t-s) - 2\rho_\delta(t-s) + \rho_\delta(t-\Delta t-s)}{(\Delta t)^2}ds\Big)g_j\Big| \\
&\leqslant \|G\|_\infty\sum_{j=-\infty}^{\infty}\int_{s_{j-1}}^{s_j}\frac{|\rho_\delta(t+\Delta t-s) - 2\rho_\delta(t-s) + \rho_\delta(t-\Delta t-s)|}{(\Delta t)^2}ds \\
&= \|G\|_\infty\sum_{j=-\eta}^{\eta}\int_{s_{j-1}}^{s_j}\frac{|\rho_\delta(\Delta t-y) - 2\rho_\delta(-y) + \rho_\delta(-\Delta t-y)|}{(\Delta t)^2}dy,
\end{aligned}$$

where $\eta = \left[p\dfrac{\delta}{\Delta t}\right] + 1$. So, we obtain

$$|D_\delta^2(G)| \quad \le \quad \frac{\|G\|_\infty}{(\Delta t)^2}\sum_{j=-\eta}^{\eta}\int_{s_{j-1}}^{s_j}|\mathrm{d}^*(y)|dy,$$

where

$$\begin{aligned} \mathrm{d}^*(y) &= \rho_\delta(-(y-\Delta t)) - 2\rho_\delta(-y) + \rho_\delta(-(y+\Delta t)) \\ &= \int_0^{\Delta t}\int_{-\Delta t}^0 \rho_\delta''(-(y+\xi_1+\xi_2))d\xi_1\xi_2, \end{aligned}$$

and

$$\rho_\delta''(x) = \frac{A_p}{\delta}\Big(-\frac{2}{\delta^2}\exp(-\frac{x^2}{\delta^2}) + \frac{4x^2}{\delta^4}\exp(-\frac{x^2}{\delta^2})\Big).$$

Therefore, we have (see [20])

$$\begin{aligned} |D_\delta^2(G)| &\leq \frac{\|G\|_\infty}{(\Delta t)^2}\int_0^{\Delta t}\int_{-\Delta t}^0 \Big(\sum_{j=-\eta}^{\eta}\int_{s_{j-1}}^{s_j} |\rho_\delta''(-(y+\xi_1+\xi_2))|dy\Big)d\xi_1\xi_2 \\ &= \frac{\|G\|_\infty}{(\Delta t)^2}\int_0^{\Delta t}\int_{-\Delta t}^0 \int_{-p\delta-(\xi_1\xi_2)}^{p\delta-(\xi_1\xi_2)} |\rho_\delta''(-(y+\xi_1+\xi_2))|dyd\xi_1\xi_2 \leq \frac{C\|G\|_\infty}{\delta^2(\Delta t)^2}. \end{aligned}$$

□

Suppose the exact function η, in the additional condition (1. 4), is not available, but a perturbed version η^ε is at hand. By applying the described method, we get $\check{\eta}(t) = \mathcal{J}_\delta\eta^\varepsilon(t)$, where $\check{\eta}$ is the mollified version of η and δ is called the radius of mollification. In the rest, we use $\check{\eta}$ in our numerical computations. Moreover, we will use the mollification technique to find a stable estimation of Caputo's derivative.

2.2. The finite difference algorithm.

Now, we present a numerical scheme to solve the problem (1. 1)-(1. 4). For this purpose, we separate (1. 1)-(1. 4) into two subproblem. The first subproblem is a direct problem as:

$$\begin{aligned} D_t^{(\alpha)}u(x,t) &= u_{xx}(x,t) + f(x,t), & (x,t) &\in [0,\bar{x}]\times[0,1], & (2.\ 7)\\ u(x,0) &= \phi(x), & x &\in [0,\bar{x}], & (2.\ 8)\\ u_t(x,0) &= \psi(x), & x &\in [0,\bar{x}], & (2.\ 9)\\ u(0,t) &= \varphi(t), & t &\in [0,1], & (2.\ 10)\\ u(\bar{x},t) &= \eta(t), & t &\in [0,1], & (2.\ 11) \end{aligned}$$

because it has known initial and boundary conditions. Another subproblem is the following inverse problem:

$$\begin{aligned} D_t^{(\alpha)}u(x,t) &= u_{xx}(x,t) + f(x,t), & (x,t) &\in [\bar{x},1]\times[0,1], & (2.\ 12)\\ u(x,0) &= \phi(x), & x &\in [\bar{x},1], & (2.\ 13)\\ u_t(x,0) &= \psi(x), & x &\in [\bar{x},1], & (2.\ 14)\\ u(\bar{x},t) &= \eta(t), & t &\in [0,1], & (2.\ 15)\\ u(1,t) &= \rho(t), & t &\in [0,1]. & (2.\ 16) \end{aligned}$$

Suppose

$$\begin{aligned} x_i &= ih, & i &= 0,1,...,M,\\ t_n &= nk, & n &= 0,1,...,N, \end{aligned}$$

where M and N are positive integers, $h = \frac{1}{M}$ and $k = \frac{1}{N}$. Thus, the domian $\Omega = [0,1] \times [0,1]$ can be discretized by the mesh points (x_i, t_n). In addition, suppose

$$f_i^n = f(ih, nk),\ \varphi^n = \varphi(nk),\ \eta^n = \eta(nk),\ \phi_i = \phi(ih),\ \psi_i = \psi(ih),$$

and $\bar{x} = sh$ where $1 \leq s \leq M-1$. To obtain an implicit finite difference formula for Eq. (2. 7), we employ the discrete estimations to the time and space derivative terms which have been given in [32] as:

$$u_t(x_i, t_n) = \frac{1}{k}(u_i^{n+1} - u_i^n) + O(k), \tag{2. 17}$$

$$\delta_{xx} u_i^n := u_{xx}(x_i, t_n) = \frac{1}{h^2}(u_{i-1}^n - 2u_i^n + u_{i+1}^n) + O(h^2). \tag{2. 18}$$

where $u_i^n = u(x_i, t_n)$.

The Riemann-Liouville fractional integral operator J_t of order $\mu > 0$ is defined as [22]:

$$J_t^{(\mu)} f(x,t) = \frac{1}{\Gamma(\mu)} \int_0^t (t-s)^{\mu-1} f(x,s) ds.$$

Applying the operator $J_t^{(\alpha-1)}$ on the two sides of Eq. (2. 7) results [10]:

$$u_t(x,t) = \psi(x) + \frac{1}{\Gamma(\alpha-1)} \int_0^t \frac{\partial^2 u(x,s)}{\partial x^2} \frac{ds}{(t-s)^{2-\alpha}} + F(x,t), \tag{2. 19}$$

where $F(x,t) = J_t^{(\alpha-1)} f(x,t)$. Using Eqs. (2. 17) and (2. 18), we obtain the following finite difference scheme for Eq. (2. 19) as

$$u_i^{n+1} - u_i^n = k\psi_i + \gamma \sum_{j=0}^{n+1} \omega_j^{(\alpha)} \delta_{xx} u_i^{n-j+1} + kF_i^{n+1}, \tag{2. 20}$$

where $\gamma = \frac{k^\alpha}{h^2}$, $\omega_0^{(\alpha)} = 1$ and

$$\omega_j^{(\alpha)} = \frac{(-1)^j \Gamma(2-\alpha)}{\Gamma(j+1)\Gamma(2-\alpha-j)},\ \ j \geq 1.$$

Also,

$$F_i^{n+1} = k^{\alpha-1} \sum_{j=0}^{n+1} \omega_j^{(\alpha)} f_i^{n-j+1} + O(k).$$

Now, we give a numerical scheme for solving the direct subproblem (2. 7)-(2. 11). By using Eq. (2. 20), for $i = 1, ..., s-1$ and $n = 0, 1, ..., N-1$, we have

$$-\gamma u_{i-1}^1 + (1+2\gamma)u_i^1 - \gamma u_{i+1}^1 = u_i^0 + k\psi_i + kF_i^1, \tag{2. 21}$$

for $n = 0$, and

$$-\gamma u_{i-1}^{n+1} + (1+2\gamma)u_i^{n+1} - \gamma u_{i+1}^{n+1} = u_i^n + \gamma \sum_{j=1}^{n+1} \omega_j^{(\alpha)} \delta_{xx} u_i^{n-j+1} + k\psi_i + kF_i^{n+1}, \tag{2. 22}$$

for $n \geq 1$, with the initial temperature distribution

$$u_i^0 = \phi_i, \quad i = 0, 1, ..., s,$$

and

$$u_0^n = \varphi^n, \quad u_s^n = \eta^n, \quad n = 1, 2, ..., N.$$

Using Eqs. (2. 21)-(2. 22), for $i = 1, ..., s-1$ and $n = 0, 1, ..., N-1$, we obtain the following matrix form

$$\mathbf{A}\mathbf{U}^1 = \mathbf{U}^0 + \Psi + \mathbf{F}^1, \tag{2. 23}$$

in which

$$\mathbf{A} = \begin{pmatrix} 1+2\gamma & -\gamma & 0 & 0 & 0 & \cdots & 0 \\ -\gamma & 1+2\gamma & -\gamma & 0 & 0 & \cdots & 0 \\ 0 & -\gamma & 1+2\gamma & -\gamma & 0 & \cdots & 0 \\ \vdots & \vdots & \vdots & \vdots & \vdots & \vdots & \\ 0 & 0 & 0 & \cdots & -\gamma & 1+2\gamma & -\gamma \\ 0 & 0 & 0 & \cdots & 0 & -\gamma & 1+2\gamma \end{pmatrix}_{(s-1)\times(s-1)},$$

$$\mathbf{B} = \begin{pmatrix} 1 & -2 & 1 & 0 & 0 & \cdots & 0 \\ 0 & 1 & -2 & 1 & 0 & \cdots & 0 \\ \vdots & \vdots & \ddots & \ddots & \ddots & & \vdots \\ 0 & 0 & \cdots & 0 & 1 & -2 & 1 \end{pmatrix}_{(s-1)\times(s+1)},$$

$\mathbf{U}^0 = (u_1^0, u_2^0, ..., u_{s-1}^0)^t$, $\mathbf{U}^1 = (u_1^1, u_2^1, ..., u_{s-1}^1)^t$, $\Psi = k(\psi_1, \psi_2, ..., \psi_{s-1})^t$ and

$$\mathbf{F}^1 = k(F_1^1, F_2^1, ..., F_{s-1}^1)^t,$$

where the superindex t denotes the transposition. Also, for $n \geq 1$, from (2. 22) we have

$$\mathbf{A}\mathbf{U}^{n+1} = \mathbf{U}^n + \gamma \sum_{j=1}^{n+1} \omega_j^{(\alpha)} \mathbf{B}\bar{\mathbf{U}}^{n-j+1} + \Psi + \mathbf{F}^{n+1}, \tag{2. 24}$$

in which

$$\begin{aligned} \mathbf{U}^n &= (u_1^n, u_2^n, ..., u_{s-1}^n)^t, \\ \mathbf{U}^{n+1} &= (u_1^{n+1}, u_2^{n+1}, ..., u_{s-1}^{n+1})^t, \\ \bar{\mathbf{U}}^j &= (u_0^j, u_1^j, ..., u_{s-1}^j, u_s^j)^t, \end{aligned}$$

$\Psi = k(\psi_1, \psi_2, ..., \psi_{s-1})^t$ and $\mathbf{F}^{n+1} = k(F_1^{n+1}, F_2^{n+1}, ..., F_{s-1}^{n+1})^t$. The linear systems (2. 23) and (2. 24) give the approximate solution of (2. 7)-(2. 11).

Now, we find the numerical solution of the inverse subproblem (2. 12)-(2. 16). To this end, we apply the proposed scheme for $i = s+1, ..., M$ and $n = 1, 2, ..., N$. Suppose $\upsilon = \mathcal{J}_\delta u$ is the mollified version of u and the value of $\upsilon(x,t)$ at (x_i, t_n) is indicated by U_i^n. In addition, suppose

$$W_i^n = \upsilon_x(ih, nk), \; Q_i^n = D_t^{(\alpha)} \upsilon(ih, nk), \; f_i^n = f(ih, nk), \; \check{\eta}_n = \check{\eta}(nk).$$

Notice that

$$U_s^n = \check{\eta}_n, \quad Q_s^n = D_t^{(\alpha)}(\check{\eta}_n), \quad n = 1, 2, ...N,$$

and

$$U_i^0 = \phi_i, \quad i = s, s+1, ..., M.$$

It should be noted that u_{s-1}^n can be obtained from the solution of the direct subproblem. So, we can approximate $\upsilon_x(\bar{x}, t)$ at the node points as

$$W_s^n = \frac{1}{h}(\check{\eta}_n - u_{s-1}^n), \quad n = 1, 2, ..., N.$$

Now, the approximate solution of (2. 12)-(2. 16) can be found by the finite difference marching scheme

$$U_{i+1}^n = U_i^n + hW_i^n, \tag{2. 25}$$

$$W_{i+1}^n = W_i^n + h(Q_i^n - f_i^n), \tag{2. 26}$$

$$Q_{i+1}^n = D_t^{(\alpha)}(\mathcal{J}_{\delta_{i+1}} U_{i+1}^n). \tag{2. 27}$$

where $i = s, ..., M-1$ and $n = 1, 2, ..., N$.
In (2. 27), let $\vartheta_i^n := \mathcal{J}_{\delta_i} U_i^n$ at each level i for $n \in \{0, 1, ..., N\}$. The discrete computed fractional order derivative, denoted by $D_t^{(\alpha)}\vartheta_i^n$ in the grid points, will be as [28]

$$D_t^{(\alpha)}\vartheta_i^n = \frac{k^{-\alpha}}{\Gamma(3-\alpha)} \sum_{r=0}^{j-1} d_{j,r}(\vartheta_i^{r+2} - 2\vartheta_i^{r+1} + \vartheta_i^r) + O(k), \tag{2. 28}$$

where $d_{j,r} = (j-r)^{2-\alpha} - (j-r-1)^{2-\alpha}$.

3. Stability and convergence

In the present section, we prove that the finite difference scheme (2. 25)-(2. 27) for numerical solving of the inverse problem (2. 12)-(2. 16) is stable and convergent.

Theorem 3.1. *(Stability of the marching algorithm) Suppose $|U_i|$, $|W_i|$, $|Q_i|$ are maximum values of $|U_i^n|$, $|W_i^n|$, $|Q_i^n|$, where $n = 0, 1, ..., N$. For the marching scheme (2. 25)-(2. 27), there exist two constants θ_1 and θ_2, such that*

$$\max\{|U_M|, |W_M|, |Q_M|\} \leq \theta_1 \max\{|U_s|, |W_s|, |Q_s|\} + \theta_2.$$

Proof. Let $M_f = \max_{x,t \in [0,1]}\{|f(x,t)|\}$. By using (2. 25) and (2. 26), we have

$$|U_{i+1}^n| \leq (1+h)\max\{|U_i^n|, |W_i^n|\}, \tag{3. 29}$$

$$|W_{i+1}^n| \leq (1+h)\max\{|W_i^n|, |Q_i^n|\} + hM_f. \tag{3. 30}$$

From (2. 27) and Theorem 2.3, we obtain

$$|Q_{i+1}^n| = |D_t^{(\alpha)}(\mathcal{J}_{\delta_{i+1}} U_{i+1}^n)| = \Big|\frac{1}{\Gamma(2-\alpha)} \int_0^t \frac{D^2(\mathcal{J}_{\delta_{i+1}} U_{i+1}^n)}{(t-s)^{\alpha-1}} ds\Big|$$
$$\leq \frac{1}{\Gamma(2-\alpha)} \int_0^t \frac{C\|U_{i+1}^n\|_\infty}{\delta_{i+1}^2 k^2 |(t-s)^{\alpha-1}|} ds = \frac{C(nk)^{2-\alpha}\|U_{i+1}^n\|_\infty}{\delta_{i+1}^2 k^2 \Gamma(3-\alpha)}.$$

Let $\bar{\delta} = \min_i\{\delta_i\}$. By applying (3. 29), we have

$$|Q_{i+1}^n| \leq \frac{C(nk)^{2-\alpha}(1+h)}{\bar{\delta}^2 k^2 \Gamma(3-\alpha)} \max\{|U_i^n|, |W_i^n|\}. \tag{3. 31}$$

Also, let

$$\hat{C} = \max\Big\{1, \frac{C(nk)^{2-\alpha}}{\bar{\delta}^2 k^2 \Gamma(3-\alpha)}\Big\}.$$

From (3. 29)-(3. 31), we obtain

$$\max\{|U_{i+1}|, |W_{i+1}|, |Q_{i+1}|\} \leq (\hat{C} + h\hat{C}) \max\{|U_i|, |W_i|, |Q_i|\} + hM_f.$$

Iterating this inequality $M - s$ times, we get

$$\max\{|U_M|, |W_M|, |Q_M|\} \leq (\hat{C} + h\hat{C})^{M-s} \max\{|U_s|, |W_s|, |Q_s|\} + \tau h M_f,$$

where $\tau = \sum_{i=0}^{M-s-1} (\hat{C} + h\hat{C})^i$. This inequality implies

$$\max\{|U_M|, |W_M|, |Q_M|\} \leq \hat{C}^{M-s} \exp(1) \max\{|U_s|, |W_s|, |Q_s|\} + \tau h M_f.$$

Letting $\theta_1 = \hat{C}^{M-s} \exp(1)$ and $\theta_2 = \tau h M_f$ complete the proof of stability. □

Theorem 3.2. *The finite difference marching scheme (2. 25)-(2. 27) is convergent.*

Proof. Suppose $i \in \{s+1, ..., M\}$ and $n \in \{0, 1, ..., N\}$. First, we define the discrete error functions $\Delta U_i^n = U_i^n - u(ih, nk)$ and $\Delta W_i^n = W_i^n - u_x(ih, nk)$. By applying Theorem 2.2, we have

$$\begin{aligned} |Q_i^n - D_t^{(\alpha)} u(ih, nk)| &= |D_t^{(\alpha)}(\mathcal{J}_{\delta_i} U_i^n) - D_t^{(\alpha)} u(ih, nk) + O(k)| \\ = |D_t^{(\alpha)}(U_i^n - u(ih, nk)) + O(k)| &\leq \frac{1}{\Gamma(2-\alpha)} \int_0^{nk} \frac{C\varepsilon}{\delta_i^2 (nk-s)^{\alpha-1}} ds + O(k) \\ = \frac{C\varepsilon (nk)^{2-\alpha}}{\delta_i^2 \Gamma(3-\alpha)} + O(k) &\leq \frac{C\varepsilon}{\delta_i^2 \Gamma(3-\alpha)} + O(k) = C_\alpha \frac{\varepsilon}{\delta_i^2} + O(k), \end{aligned} \tag{3. 32}$$

where $C_\alpha = \dfrac{C}{\Gamma(3-\alpha)}$.

Expanding the exact solution $u(x,t)$ by the Taylor series, we obtain

$$u((i+1)h, nk) = u(ih, nk) + h u_x(ih, nk) + O(h^2), \tag{3. 33}$$

$$u_x((i+1)h, nk) = u_x(ih, nk) + h(D_t^{(\alpha)} u(ih, nk) - f(ih, nk)) + O(h^2), \tag{3. 34}$$

From (2. 25) and (3. 33), we have

$$\begin{aligned} \Delta U_{i+1}^n &= U_{i+1}^n - u((i+1)h, nk) \\ &= U_i^n + hW_i^n - u((i+1)h, nk) \\ &= U_i^n + hW_i^n - u(ih, nk) - hu_x(ih, nk) + O(h^2) \\ &= (U_i^n - u(ih, nk)) + h(W_i^n - u_x(ih, nk)) + O(h^2) \\ &= \Delta U_i^n + h\Delta W_i^n + O(h^2). \end{aligned}$$

So, we result

$$|\Delta U_{i+1}^n| \leq |\Delta U_i^n| + h|\Delta W_i^n| + O(h^2). \tag{3. 35}$$

By using (2. 26), (3. 32) and (3. 34), we have

$$\begin{aligned}
\Delta W_{i+1}^n &= W_{i+1}^n - u_x((i+1)h, nk) \\
&= W_i^n + h(Q_i^n - f_i^n) - u_x((i+1)h, nk) \\
&= W_i^n + h(Q_i^n - f_i^n) - u_x(ih, nk) - h(D_t^{(\alpha)}u(ih, nk) - f(ih, nk)) + O(h^2) \\
&= W_i^n - u_x(ih, nk) + h(Q_i^n - D_t^{(\alpha)}u(ih, nk)) + O(h^2) \\
&= \Delta W_i^n + hC_\alpha \frac{\varepsilon}{\delta_i^2} + O(hk) + O(h^2).
\end{aligned}$$

So, we get

$$|\Delta W_{i+1}^n| \leq |\Delta W_i^n| + hC_\alpha \frac{\varepsilon}{\delta_i^2} + O(hk) + O(h^2). \tag{3. 36}$$

Let $|\Delta U_i| = \max\limits_{0 \leq n \leq N} |\Delta U_i^n|$ and $|\Delta W_i| = \max\limits_{0 \leq n \leq N} |\Delta W_i^n|$. Thus, from (3. 35), (3. 36), we obtain

$$\begin{aligned}
|\Delta U_{i+1}| &\leq |\Delta U_i| + h|\Delta W_i| + O(h^2), \\
|\Delta W_{i+1}| &\leq |\Delta W_i| + hC_\alpha \frac{\varepsilon}{\delta_i^2} + O(hk) + O(h^2).
\end{aligned}$$

Let $\hat{\delta} = \min\limits_i\{\delta_i\}$, hence

$$\begin{aligned}
|\Delta U_{i+1}| &\leq (1+h)\max\{|\Delta U_i|, |\Delta W_i|\} + O(h^2), \\
|\Delta W_{i+1}| &\leq \max\{|\Delta W_i|\} + hC_\alpha \frac{\varepsilon}{\hat{\delta}^2} + O(hk) + O(h^2),
\end{aligned}$$

and

$$\max\{|\Delta U_{i+1}|, |\Delta W_{i+1}|\} \leq (1+h)\max\{|\Delta U_i|, |\Delta W_i|\} + \Lambda,$$

where $\Lambda = hC_\alpha \frac{\varepsilon}{\hat{\delta}^2} + O(hk) + O(h^2)$. Now, suppose $\Delta_i = \max\{|\Delta U_i|, |\Delta W_i|\}$. Thus, we have

$$\Delta_{i+1} \leq (1+h)\Delta_i + \Lambda,$$

and

$$\begin{aligned}
\Delta_M &\leq (1+h)\Delta_{M-1} + \Lambda \\
&\leq (1+h)^2\Delta_{M-2} + (1+h)\Lambda + \Lambda \\
&\leq ... \leq (1+h)^{M-s}\Delta_s + \tau\Lambda,
\end{aligned}$$

where $\tau = \sum_{i=0}^{M-s-1}(1+h)^i$. Now, by using Theorem 2.1, for $n \in \{0, 1, ..., N\}$, there exists constants C_n and D_n, such that

$$\begin{aligned}
|\Delta U_s^n| &= |U_s^n - u(sh, nk)| \leq C_n\delta + \varepsilon, \\
|\Delta W_s^n| &= |W_s^n - u_x(sh, nk)| \leq D_n\delta + \varepsilon.
\end{aligned}$$

Let $C^{'} = \max\{C_n, D_n|\, n = 0, ..., N\}$, then we have

$$\Delta_s = \max\{|\Delta U_s^n|, |\Delta W_s^n|\} \leq C^{'}\delta + \varepsilon,$$

and

$$\Delta_M \leq \exp(1)(C^{'}\delta + \varepsilon) + \tau\Lambda.$$

As a result, by choosing $\hat{\delta} = \hat{\delta}(\varepsilon)$, when ε, h and k tend towards 0, δ and Λ tend towards 0. Thus, Δ_M will tend to 0. It completes the proof. □

4. Numerical implementation

The present section is dedicated to investigating the ability of the introduced algorithm. To simulate the data for the inverse problem, some random noises are added to the data resulted from the function $\eta(t)$, in the additional condition (1. 4). Suppose that ε is a noise level. For generating noisy data, the relation

$$\eta^{\varepsilon}(t_i) = \eta(t_i)(1 + \varepsilon \times rand(i)),$$

will be used, where $rand(i)$ is a uniformly distributed random number in $[-1, 1]$. Also, to demonstrate the accuracy of our method, by using the L^2-norm, we define

$$E_{L_2}(h,k) = \max_{1\le n\le N} \|u^n - U^n\|.$$

We calculate the convergence order of the proposed method with the following formulas

$$Order(h) = \log_{\frac{h_1}{h_2}} \Big(\frac{E_{L_2}(h_1,k)}{E_{L_2}(h_2,k)}\Big), \qquad Order(k) = \log_{\frac{k_1}{k_2}} \Big(\frac{E_{L_2}(h,k_1)}{E_{L_2}(h,k_2)}\Big).$$

The computations are performed on a personal computer using a 2.20 GHz processor and the codes are written in Matlab R2014a.

Example 1. Consider Eq. (1. 1) with $f(x,t) = -e^x(2t^{\alpha} + \dfrac{\pi \csc(\pi\alpha)}{\Gamma(-\alpha)})$. Also, let $\phi(x) = \psi(x) = 0$, $\varphi(t) = t^{\alpha}$ and $\rho(t) = e^1 t^{\alpha}$. The exact solution of this problem is $u(x,t) = t^{\alpha} e^x$.

Figure 1 shows the exact and the estimated solutions for $\rho(t)$ with regularization and without regularization when $\alpha = 1.5$, $\bar{x} = 0.65$, $M = 200$, $N = 150$ and $\varepsilon = 1\%, 5\%, 10\%, 15\%$. Furthermore, Figure 2 shows the exact and the estimated solutions to $\rho(t)$ for values $\alpha = 1.2, 1.4, 1.6, 1.8$ when $\bar{x} = 0.65$, $M = 200$, $N = 100$ and $\varepsilon = 1\%, 10\%, 20\%$.

Now, we test the errors in the sense of the L_2-norm of the numerical solutions under various time and space steps. First, the temporal errors and convergence orders are investigated by fixing $\bar{x} = 0.5$ and $M = 100$ and letting N vary. Table 1 presents the maximum L_2-norm errors and convergence orders of the method. From which we can see that, in the presence of noise, the numerical errors are decreasing as the mesh is refined. Also, the convergence orders are more than 1. Next, we investigate the numerical accuracies of the method in space. The computational results, when $N = 100$, are listed in Table 2. It can be seen from the table that for various noise levels, by increasing the number of space steps, the errors are decreased. Also, the convergence orders become more than 1.5. So we can expect these values converge to 2 when the number of steps is increased. Those are in good agreement with the theoretical results.

Figure 3 shows the exact and numerical approximation of $u(x,t)$ when $\alpha = 1.5, \bar{x} = 0.5, M = 200, N = 200$ and $\varepsilon = 10\%$. Finally, Figure 4 displays the absolute error function for the estimated solution when $\varepsilon = 1\%$.

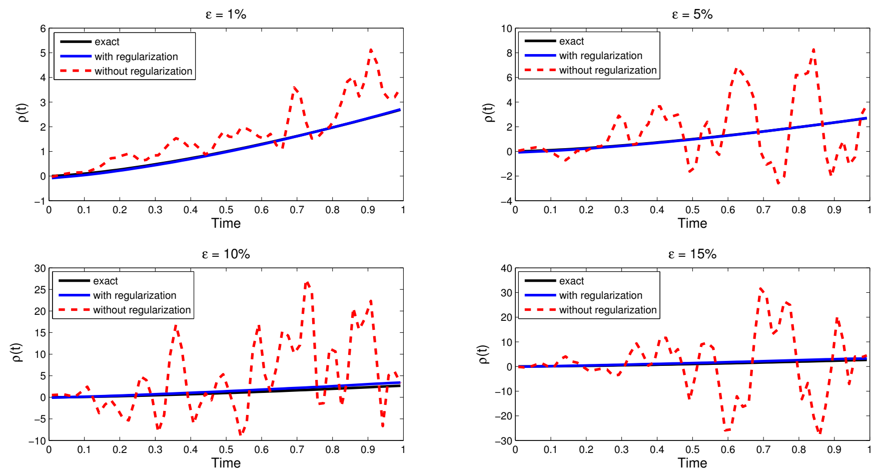

FIGURE 1. The function $\rho(t)$ and its numerical values without regularization and with regularization in Example 1 when $\alpha = 1.5$.

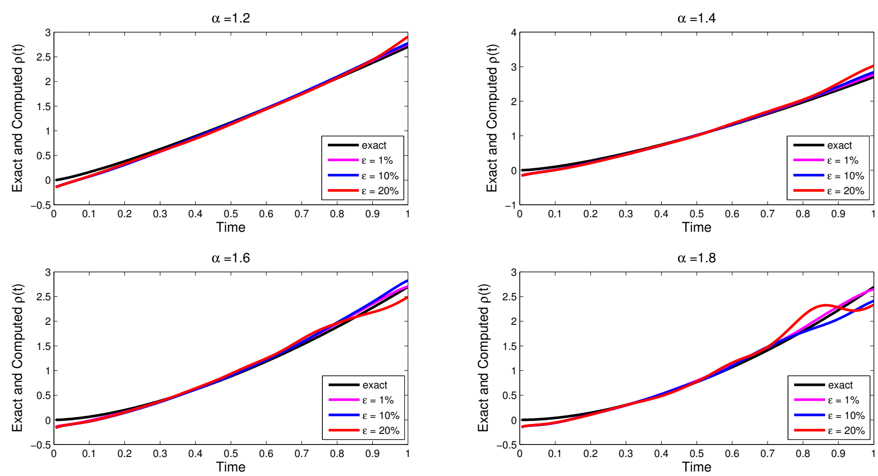

FIGURE 2. The function $\rho(t)$ and its numerical estimations in Example 1 for different values of α and ε when $\bar{x} = 0.65$.

Example 2. In this example, we consider the inverse problem associated with the direct problem

$$\begin{aligned}
&D_t^{(\alpha)} u(x,t) = u_{xx}(x,t),\\
&u(x,0) = u_t(x,0) = 0,\\
&u(0,t) = 0,\\
&u(1,t) = \begin{cases} t, & 0 \leqslant t \leqslant \frac{1}{2},\\ 1-t, & \frac{1}{2} < t \leqslant 1. \end{cases}
\end{aligned}$$

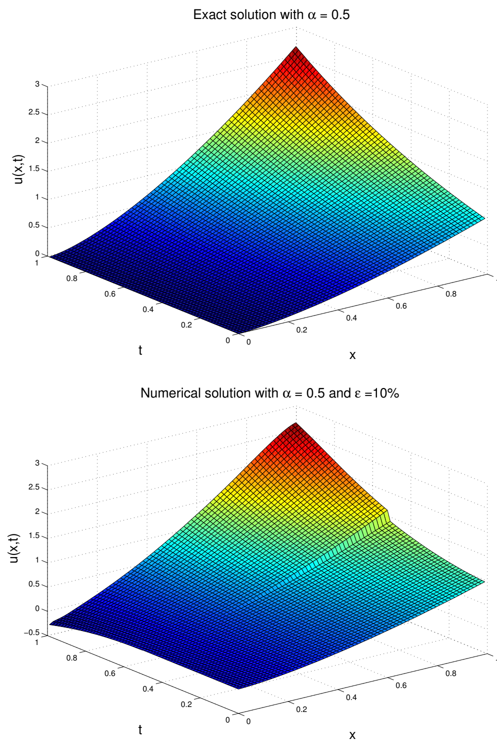

FIGURE 3. The exact and numerical solution for Example 1 when $\alpha = 1.5, \bar{x} = 0.5$ and $\varepsilon = 10\%$.

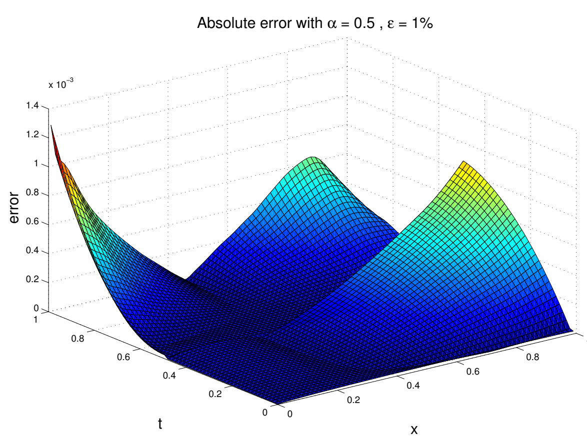

FIGURE 4. The absolute error function for numerical solution of Example 1 when $\alpha = 1.5, \bar{x} = 0.5$ and $\varepsilon = 1\%$.

TABLE 1. The maximum L_2-norm errors and convergence orders for Example 1 when $M = 100$.

α	N	E_{L_2}	$Order(k)$	E_{L_2}	$Order(k)$	E_{L_2}	$Order(k)$
		$\varepsilon = 1\%$		$\varepsilon = 5\%$		$\varepsilon = 10\%$	
1.25	64	0.0991	$*$	0.1187	$*$	0.1291	$*$
	128	0.0724	1.3688	0.0863	1.3754	0.0921	1.4017
	256	0.0525	1.3790	0.0621	1.3897	0.0652	1.4126
	512	0.0379	1.3852	0.0446	1.3924	0.0456	1.4298
1.5	64	0.1053	$*$	0.1263	$*$	0.1401	$*$
	128	0.0760	1.3855	0.0904	1.3971	0.0986	1.4209
	256	0.0544	1.3971	0.0642	1.4081	0.0687	1.4352
	512	0.0387	1.4057	0.0454	1.4141	0.0475	1.4463
1.75	64	0.1166	$*$	0.1371	$*$	0.1570	$*$
	128	0.0831	1.4031	0.0961	1.4266	0.1095	1.4338
	256	0.0584	1.4229	0.0672	1.4301	0.0751	1.4581
	512	0.0409	1.4303	0.0465	1.4452	0.0511	1.4697

TABLE 2. The maximum L_2-norm errors and convergence orders for Example 1 when $N = 100$.

α	M	E_{L_2}	$Order(h)$	E_{L_2}	$Order(h)$	E_{L_2}	$Order(h)$
		$\varepsilon = 1\%$		$\varepsilon = 5\%$		$\varepsilon = 10\%$	
1.25	64	0.0945	$*$	0.1101	$*$	0.1313	$*$
	128	0.0667	1.4168	0.0763	1.4430	0.0883	1.4870
	256	0.0452	1.4757	0.0511	1.4932	0.0576	1.5330
	512	0.0306	1.5359	0.0331	1.5438	0.0368	1.5652
1.5	64	0.1044	$*$	0.1247	$*$	0.1436	$*$
	128	0.0721	1.4480	0.0831	1.5006	0.0941	1.5260
	256	0.0480	1.5021	0.0535	1.5533	0.0601	1.5657
	512	0.0311	1.5434	0.0340	1.5735	0.0376	1.5984
1.75	64	0.1167	$*$	0.1296	$*$	0.1493	$*$
	128	0.0782	1.4923	0.0852	1.5211	0.0971	1.5376
	256	0.0511	1.5303	0.0546	1.5604	0.0619	1.5687
	512	0.0324	1.5772	0.0342	1.5965	0.0383	1.6162

Here, we do not have the analytic solution of the problem. Thus, we will use the approximate solution of the direct problem, obtained by the numerical scheme proposed in Section 2, as an exact solution. Then, the additional data $\eta(t)$ will be found by using this supposed exact solution, although it contains some computational errors.

Figure 5 shows the function $\rho(t)$ and its estimations, with regularization and without regularization when $\alpha = 1.5$, $\bar{x} = 0.7$, $M = 200$, $N = 200$ and $\varepsilon = 1\%, 5\%, 10\%, 15\%$. Also, Figure 6 shows the exact and the estimated solutions to $\rho(t)$ for several values of $\alpha = 1.3, 1.6$ when $\bar{x} = 0.65$, $M = N = 200$ and $\varepsilon = 1\%, 5\%, 10\%, 15\%$.

Now, we investigate the spatial and temporal errors and convergence orders. Let $\bar{x} = 0.5$ and $M = 100$. Table 3 presents errors and convergence orders for different time

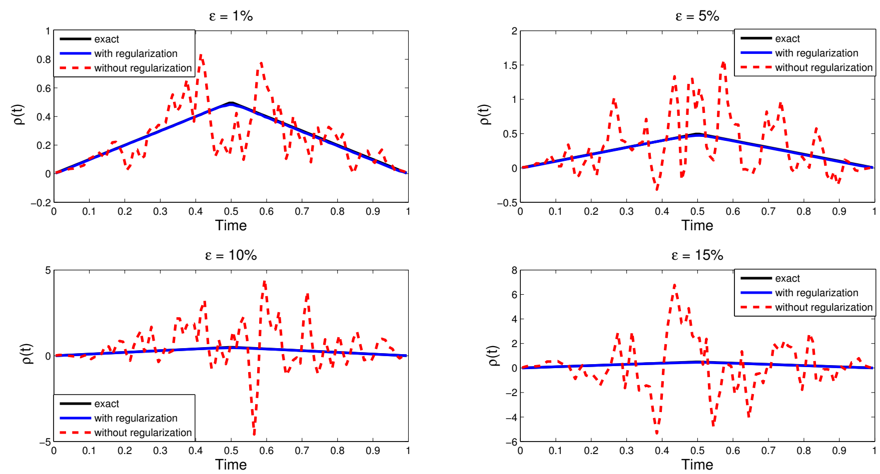

FIGURE 5. The function $\rho(t)$ and its numerical approximations without regularization and with regularization in Example 2 when $\alpha = 1.5$.

TABLE 3. The maximum L_2-norm errors and convergence orders for Example 2 when $M = 100$.

α	N	E_{L_2}	$Order(k)$	E_{L_2}	$Order(k)$	E_{L_2}	$Order(k)$
		$\varepsilon = 1\%$		$\varepsilon = 5\%$		$\varepsilon = 10\%$	
1.25	64	0.0271	$*$	0.0376	$*$	0.0442	$*$
	128	0.0169	1.6036	0.0227	1.6564	0.0260	1.7000
	256	0.0103	1.6408	0.0134	1.6940	0.0149	1.7450
	512	0.0062	1.6613	0.0078	1.7179	0.0085	1.7529
1.5	64	0.0466	$*$	0.0618	$*$	0.0801	$*$
	128	0.0285	1.6351	0.0365	1.6932	0.0457	1.7527
	256	0.0169	1.6864	0.0211	1.7299	0.0255	1.7922
	512	0.0099	1.7071	0.0120	1.7583	0.0140	1.8214
1.75	64	0.0771	$*$	0.0940	$*$	0.1061	$*$
	128	0.0456	1.6908	0.0543	1.7311	0.0591	1.7953
	256	0.0261	1.7471	0.0306	1.7745	0.0324	1.8241
	512	0.0146	1.7877	0.0168	1.8214	0.0174	1.8621

steps. Also, by fixing the time step $N = 100$, Table 4 presents errors and convergence orders in the spatial direction. It can be seen from these tables that the numerical errors are decreasing as the level of noise and the mesh size become smaller. Also, the results about the convergence orders are similar to Example 1.

TABLE 4. The maximum L_2-norm errors and convergence orders for Example 2 when $N = 100$.

α	M	E_{L_2}	$Order(h)$	E_{L_2}	$Order(h)$	E_{L_2}	$Order(h)$
		$\varepsilon = 1\%$		$\varepsilon = 5\%$		$\varepsilon = 10\%$	
1.25	64	0.0402	$*$	0.0574	$*$	0.0766	$*$
	128	0.0325	1.2369	0.0435	1.3195	0.0552	1.3877
	256	0.0236	1.3771	0.0298	1.4597	0.0370	1.4919
	512	0.0168	1.4048	0.0195	1.5282	0.0235	1.5745
1.5	64	0.0553	$*$	0.0702	$*$	0.0847	$*$
	128	0.0421	1.3135	0.0515	1.3631	0.0597	1.4188
	256	0.0297	1.4175	0.0349	1.4756	0.0388	1.5387
	512	0.0200	1.4850	0.0224	1.5580	0.0241	1.6100
1.75	64	0.0663	$*$	0.0786	$*$	0.0887	$*$
	128	0.0487	1.3614	0.0559	1.4061	0.0610	1.4541
	256	0.0333	1.4625	0.0364	1.5357	0.0393	1.5522
	512	0.0221	1.5068	0.0232	1.5690	0.0243	1.6173

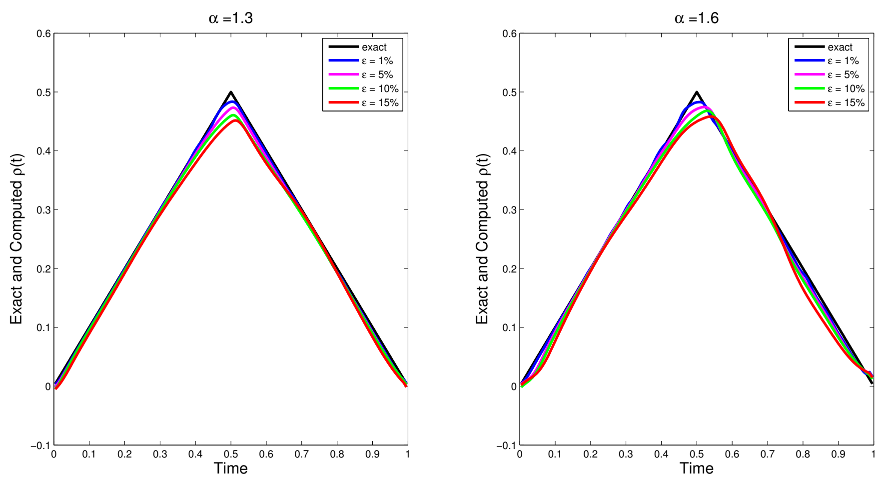

FIGURE 6. The function exact $\rho(t)$ and its numerical approximations in Example 2 for several values of α and ε when $\bar{x} = 0.65$.

5. CONCLUSION

In this work, a time-fractional inverse diffusion-wave problem for restoring an unknown boundary condition was investigated. To this aim, a numerical scheme based on the finite difference method was proposed. According to the ill-posedness of this type of inverse problems, the mollification technique was employed to compute the stabilized numerical solution. The numerical procedure was completely explained and it was proven that the presented method is stable and convergent. In the end, some test problems were surveyed to show the ability and the accuracy of the mentioned algorithm. The obtained convergence orders confirm that the convergence speed of the presented method is good, even in the presence of the noise up to fifteen percent. Therefore, the results verify the accuracy and the stability of the method.

6. ACKNOWLEDGMENTS

The authors are thankful to the reviewers and the editor for suggestions to improve the presentation of the manuscript.

REFERENCES

[1] A. Babaei and S. Banihashemi, *A stable numerical approach to solve a time-fractional inverse heat conduction problem*, Iran J. Sci. Technol. Trans. Sci. (2017) DOI:10.1007/s40995-017-0360-4.

[2] T. Batool and M. O. Ahmad, *Application of Bernstein polynomials for solving linear Volterra integro-differential equations with convolution kernels*, Punjab Univ. j. math. **49**, No. 3 (2017) 65-75.

[3] E. Bazhlekova and I. Bazhlekova, *Stokes First Problem for Viscoelastic Fluids with a Fractional Maxwell Model*, Fractal Fract **1**, No. 1 (2017) 7.

[4] D. A. Benson, S. W. Wheatcraft and M. M. Meerschaert, *The fractional-order governing equation of Levy motion*, Water Resour. Res. **36**, (2000) 1413-1423.

[5] R. Brociek, D. Slota, M. Krol, G. Matula and W. Kwasny, *Modeling of heat distribution in porous aluminum using fractional differential equation*, Fractal and Fractional **1**, No. 1 (2017) 17.

[6] M. Caputo and M. Fabrizio, *The kernel of the distributed order fractional derivatives with an application to complex materials*, Fractal Fract **1**, No. 1 (2017) 13.

[7] F. Haq, K. Shah, A. Khan, M. Shahzad and G. ur Rahman, *Numerical solution of fractional order epidemic model of a vector born disease by laplace adomian decomposition method*, Punjab Univ. j. math. **49**, No. 2 (2017) 13-22.

[8] Y. C. Hon and T. Wei, *The method of fundamental solutions for solving multidimensional inverse heat conduction problems*, Computer Modeling in Engineering and Sciences **7**, No. 2 (2005) 119-132.

[9] M. R. Hooshmandasl, M. H. Heydari and C. Cattani, *Numerical solution of fractional sub-diffusion and time-fractional diffusion-wave equations via fractional-order Legendre functions*, The European Physical Journal Plus **131**, No. 8 (2016) 131-268.

[10] J. Huang, Y. Tang, L. Vazquez and J. Yang, *Two finite difference schemes for time fractional diffusion-wave equation*, Numer Algor **64**, No. 4 (2013) 707-720.

[11] M. Hussain, *Application of the Srivastav-Owa fractional calculus operator to Janowski spiral-like functions of complex order*, Punjab Univ. j. math. **50**, No. 2 (2018) 33-43.

[12] H. Jafari, *Numerical solution of time-fractional Klein-Gordon equation by using the decomposition methods*, J. Comput. Nonlinear Dynam. **11**, No. 4 (2016) 410–415.

[13] B. Jin and W Rundell, *A tutorial on inverse problems for anomalous diffusion processes*, Inverse Problems **31**, No. 3 (2015) 035003.

[14] K. Karimi, M. Alipour and M. Khaksarfard, *Numerical solution of nonlocal parabolic partial differential equation via bernstein polynomial method*, Punjab Univ. j. math. **48**, No. 1 (2016) 47-53.

[15] F. Mainardi, *Fractals and Fractional Calculus Continuum Mechanics*, Springer, Berlin, 1997.

[16] F. Mainardi, *Fractional Calculus and Waves in Linear Viscoelasticity: An Introduction to Mathematical Models*, Imperial College Press, London, 2010.

[17] C. E. Mejia, D. A. Murio and S. Zhan, *Some applications of the mollification method*. In: Lassonde, M.(ed.), Approximation, Optimization and Mathematical Economics. Physica, Heidelberg, (2001) 213-222.

[18] D. A. Murio and C. E. Mejia, *Generalized time fractional IHCP with Caputo fractional derivatives*, J. Phys: Conference Series **135**, (2008) 1-8.

[19] D. A. Murio, *Implicit finite difference approximation for time fractional diffusion equations*, Computers and Mathematics with Applications **56**, (2007) 1138-1145.

[20] D. A. Murio, *Mollification and space marching*, in: K. Woodbury (Ed.), Inverse Engineering Handbook, CRC Press, Boca Raton FL, 2002.

[21] D. A. Murio, *On the stable numerical evaluation of Caputo fractional derivatives*, Computers and Mathematics with Applications **51**, (2006) 1539-1550.
[22] I. Podlubny, *Fractional Differential Equations*, Academic Press, New York, 1999.
[23] M. I. Qadir and N. Shiraz, *A numerical treatment for the stability of josephson vortices in BEC*, Punjab Univ. j. math. **49**, No. 3 (2017) 89-97.
[24] N. Raza, *Application of Sobolev gradient method to solve Klein Gordon equation*, Punjab Univ. j. math. **48**, No. 2 (2016) 135-145.
[25] N. Raza, *Unsteady rotational flow of a second grade fluid with non-integer caputo time fractional derivative*, Punjab Univ. j. math. **49**, No. 3 (2017) 15-25.
[26] S. Riaz, M. Rafiq and O. Ahmad, *Non standard finite difference method for quadratic Riccati differential equation*, Punjab Univ. j. math. **47**, No. 2 (2015) 49-55.
[27] A. Shidfar and A. Babaei, *The Sinc-Galerkin method for solving an inverse parabolic problem with unknown source term*, Numer. Meth. Part. Differ. Equ. **29**, (2013) 64–78 .
[28] E. Sousa, *How to approximate the fractional derivative of order* $1 < \alpha \leq 2$, In: Proceedings of FDA'10. The 4th IFAC Workshop Fractional Differentiation and its Applications, Badajoz, Spain (2010).
[29] M. Suleman and S. Riaz, *Unconditionally stable numerical scheme to study the dynamics of Hepatitis b disease*, Punjab Univ. j. math. **49**, No. 3 (2017) 99-118.
[30] A. Taghavi, A. Babaei and A. Mohammadpour, *A stable numerical scheme for a time fractional inverse parabolic equation*, Inverse Probl Sci Eng. **25**, No. 10 (2016) 1474-1491.
[31] N. Taghizadeh and M. N. Foumani, *Using a reliable method for higher dimensional of the fractional Schrodinger equation*, Punjab Univ. j. math. **48**, No. 1 (2016) 11-18.
[32] A. Tveito and R. Winther, *Introduction to Partial Differential Equations*, Springer-Verlag, New York, 1998.
[33] F. Yang, C. L. Fu and X. X. Li, *A mollification regularization method for unknown source in time-fractional diffusion equation*, International Journal of Computer Mathematics **91**, No. 7 (2014) 1516–1534.
[34] S. B. Yuste and J. Q. Murillo, *A finite difference method with non-uniform timesteps for fractional diffusion equations*, Computer Physics Communications **183**, (2012) 2594–2600.